

**SEISMIC EVENT LOCATION: DEALING WITH MULTI-DIMENSIONAL UNCERTAINTY, MODEL  
NON-LINEARITY AND LOCAL MINIMA**

Sanford Ballard

Sandia National Laboratories

Sponsored by National Nuclear Security Administration  
Office of Nonproliferation Research and Engineering  
Office of Defense Nuclear Nonproliferation

Contract No. DE-AC04-94-AL85000

**ABSTRACT**

Seismic event location is made challenging by the difficulty of describing event location uncertainty in multi-dimensions, by the non-linearity of the Earth models used as input to the location algorithm, and by the presence of local minima which can prevent a location code from finding the global minimum. Techniques to deal with these issues will be described. Since some of these techniques are computationally expensive or require more analysis by human analysts, users need a flexible location code that allows them to select from a variety of solutions that span a range of computational efficiency and simplicity of interpretation. A new location code, LocOO, has been developed to deal with these issues.

A seismic event location is comprised of a point in 4-dimensional (4D) space-time, surrounded by a 4D uncertainty boundary. The point location is useless without the uncertainty that accompanies it. While it is mathematically straightforward to reduce the dimensionality of the 4D uncertainty limits, the number of dimensions that should be retained depends on the dimensionality of the location to which the calculated event location is to be compared. In nuclear explosion monitoring, when an event is to be compared to a known or suspected test site location, the three spatial components of the test site and event location are to be compared and 3 dimensional uncertainty boundaries should be considered. With LocOO, users can specify a location to which the calculated seismic event location is to be compared and the dimensionality of the uncertainty is tailored to that of the location specified by the user. The code also calculates the probability that the two locations in fact coincide.

The non-linear travel time curves that constrain calculated event locations present two basic difficulties. The first is that the non-linearity can cause least squares inversion techniques to fail to converge. LocOO implements a non-linear Levenberg-Marquardt least squares inversion technique that is guaranteed to converge in a finite number of iterations for tractable problems. The second difficulty is that a high degree of non-linearity causes the uncertainty boundaries around the event location to deviate significantly from elliptical shapes. LocOO can optionally calculate and display non-elliptical uncertainty boundaries at the cost of a minimal increase in computation time and complexity of interpretation.

All location codes are plagued by the possibility of having local minima obscuring the single global minimum. No code can guarantee that it will find the global minimum in a finite number of computations. Grid search algorithms have been developed to deal with this problem, but have a high computational cost. In order to improve the likelihood of finding the global minimum in a timely manner, LocOO implements a hybrid least squares-grid search algorithm. Essentially, many least squares solutions are computed starting from a user-specified number of initial locations; and the solution with the smallest sum squared weighted residual is assumed to be the optimal location. For events of particular interest, analysts can display contour plots of gridded residuals in a selected region around the best-fit location, improving the probability that the global minimum will not be missed and also providing much greater insight into the character and quality of the calculated solution.

## **OBJECTIVE**

### **Introduction**

The objective of this study is to improve our ability to locate seismic events relative to current techniques. The main areas where current practice can be improved includes the addition of capability to report 3D and 4D uncertainty information, improved handling of non-linear Earth model effects, and increasing the probability of finding global as opposed to local minima when seeking the seismic event location that best fits the available data. In addition, a new method of calculating the uncertainty ellipses around fixed-depth event location solutions is also described.

### **Multidimensional Uncertainty Boundaries.**

The linear least squares seismic event location algorithm returns two fundamental objects, examples of which are:

Final location:

```
latitude longitude    depth    origin_time
  27.4255    71.4839    37.456    894881631.266
```

4D space-time uncertainty hyper\_ellipse:

```
Principal axes:
North:  -5.13552111E-01    3.60035966E-01    3.74867000E-01    9.32939723E-01
East:   -6.33040235E-02   -9.32938424E-01    9.25246750E-01    3.60032600E-01
Depth:  -8.46798394E-01   -4.79448998E-08   -8.38960340E-03    2.72955198E-08
Time:   -1.23244918E-01    3.04267339E-07    5.76437276E-02   -2.87875086E-07
Length:  3.47029259E+01     2.08530626E+01    1.24056628E+01    4.84719957E+00
```

The first object is the seismic event location that consists of the latitude, longitude, depth and origin time that yields the smallest sum squared weighted difference, in a least squares sense, between observed and predicted seismic parameters. The second object is the uncertainty in the location, which consists of a 4D hyper-ellipse that surrounds the best-fit seismic event location. In this example, the uncertainty hyper-ellipse is represented by a 5 x 4 matrix. Each of the 4 columns of this matrix describes one of the 4 principal axes of the uncertainty hyper-ellipse. The first four elements of each column describe a 4 dimensional unit vector in Cartesian coordinates while the last element in each column describes the length of the vector in 4D space-time. The length represents the distance from the best-fit event location (the center of the hyper-ellipse) to the contour in 4D location space where the sum squared weighted residuals is greater than the sum squared weighted residuals that characterizes the best-fit location by a value of 1.

While this depiction of the uncertainty hyper-ellipse is complete, it is not particularly useful in terms of providing significant insight into the level of confidence we might have in our best-fit event location. There are two problems with it. The first is that a contour in location space where  $\chi^2 = 1$  is difficult to interpret. Fortunately, there are statistical formulas that tell us how to scale the dimensions of the hyper-ellipse such that it encompasses some desired percentage,  $p$ , of the total probability distribution (Jordan and Sverdrup, 1981; Bratt and Bache, 1988; Wilcock and Toomey, 1971, Press et al., 2002). We can point to the scaled uncertainty hyper-ellipse and state, with confidence  $p$ , that “the true location of the seismic event that generated the observations is located within this hyper-ellipse”.

The second difficulty with the uncertainty hyper-ellipse is that it is difficult to visualize and interpret a 4 dimensional surface. The key to overcoming this difficulty is careful examination of the question that is being addressed with the seismic event location and its associated uncertainty. Typically, we wish to compare our calculated event location to some other location,  $\mathbf{X}$ , in time and/or space and would like to know “did the event occur at location  $\mathbf{X}$ ”. If location  $\mathbf{X}$  has fewer than 4 dimensions, then there are components of our solution that are not relevant and those components should be ignored. The correct way to remove from consideration components of the problem that are not relevant is to project the 4D uncertainty probability distribution onto planes in location space that correspond to the irrelevant components. A detailed description of how to accomplish this mathematically is described in Press, et al. (2002).

In nuclear explosion monitoring, a frequently encountered scenario is that a seismic event is detected in general proximity to a known nuclear test site and we wish to determine whether or not the event could have occurred at the

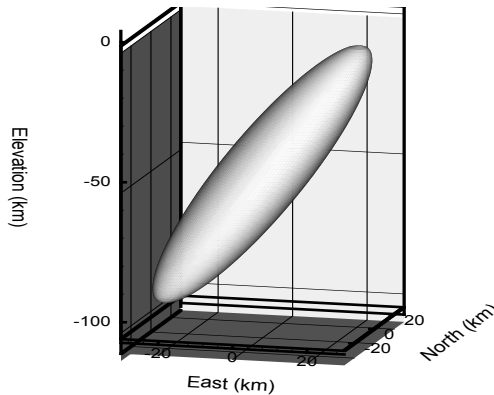


**Figure 1. A 3D uncertainty ellipsoid for a seismic event that occurred on October 25, 2002 in the Sea of Japan, viewed from the SE. The major axis of the ellipsoid plunges steeply to the W/SW, and the ellipsoid does not intersect the surface.**

test site, at some specified probability level. This is a 3 dimensional problem. The geographic coordinates and depth of the seismic event are important but the origin time of the event is not of interest. In this case, the question being asked is “does the 3D location of the test site fall within the 3D uncertainty interval centered on the seismic event location?” It is critical that all 3 components of the event and test site locations be considered jointly because the statistical analysis depends on the number of free parameters in the location comparison (Jordan and Sverdrup, 1981; Bratt and Bache, 1988). The 4D uncertainty hyper-ellipsoid returned by the least squares location algorithm should be projected onto a plane of constant time, resulting in a 3D ellipsoidal uncertainty boundary. An example of such an ellipsoid for an event that occurred in the Sea of Japan on October 25, 2002 is shown in Figure 1.

After reducing the dimensionality of the uncertainty bounds, it is useful to define a statistical index that can assist in determining the degree to which a seismic event location is co-located with a second location such as the

location of a nuclear test site. To this end, a statistic called the *co-location index* is introduced that represents the percentage of the total probability density distribution that lies outside of a surface with the shape of the uncertainty surface but scaled to pass exactly through the location of interest. If the calculated location and the location of interest coincide perfectly, then 100% of the probability density distribution lies outside of the surface and that is the value of the co-location index. If the separation between the calculated location and the location of interest is large compared to the dimensions of the uncertainty surface, the co-location index is very small. If the location of interest lies directly on the  $p\%$  confidence boundary, then the co-location index will be  $100-p$ . Note that the co-location index will be a number between 0 and 100 and will differ depending on the number of dimensions that characterize the uncertainty bound. It is appropriate to refer to the “ $n$ -dimensional co-location index”, where  $n$  ranges from one to four.

### Non-Linear Earth Models

The least squares algorithm that is at the heart of many commonly used seismic event location codes assumes that the Earth model used to generate predictions of seismic events is linear, implying that seismic travel time curves are straight lines. This is, of course, not the case and the iterative scheme originally proposed by Geiger (1910) overcomes this limitation in cases where the non-linearity is not severe. This allows the iterative least squares algorithm to find the point in 4D location space characterized by the minimum sum squared weighted residuals, in most cases. The linearity assumption also permits the calculation of the hyper-elliptical uncertainty boundaries, as discussed in the previous section. In practice, however, it frequently occurs that the non-linearity is sufficiently severe that its effects cannot be ignored. This can manifest itself in two ways: the algorithm may fail to converge, and the actual uncertainty boundaries may deviate significantly from elliptical shapes.

Figure 2 illustrates a location situation where the non-linear effects cause the least squares algorithm to fail to converge. Note that the contours of constant root mean squared weighted residuals indicated by the colors in Figure 2 are not elliptical in shape. This results from significant non-linearity of the Earth model across the Moho at a depth of 30 km. If nothing is done to prevent it, the iterative least squares algorithm will oscillate infinitely between two non-optimal solutions indicated by the purple lines and circles. The step length weighting algorithm implemented in libloc, illustrated on the right, fails to find the minimum sum squared weighted residuals after 30 iterations. The Levenberg-Marquardt algorithm implemented by LocOO (Marquardt, 1963; Levenberg, 1944; Ballard, 2002) is illustrated on the left of Figure 2. It successfully deals with the non-linearity in the following manner: for each proposed step that will result in an increase in the sum squared weighted residuals, the step length is shortened and the direction of the step is rotated such that the step moves more in the direction of steepest descent. It is guaranteed to converge in a finite number of iterations, for tractable problems.

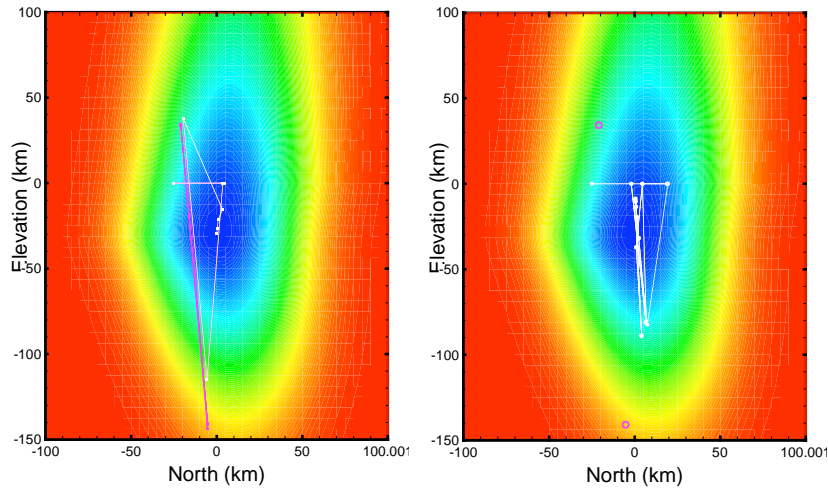


**Figure 2. Comparison of the Levenberg-Marquardt damping algorithm implemented by LocOO (left) and the step-length weighting damping algorithm implemented by libloc (right). Colors represent RMS weighted residuals at each point on a vertical slice through the hypocenter, decreasing from red to blue. White symbols connected by lines indicate the solution location trajectory followed by each algorithm. The purple lines and symbols represent the cyclical solution trajectory followed by the iterative least-squares algorithm in the case where no damping algorithm is implemented.**

The other negative impact of significant non-linearity is that the calculated uncertainty boundaries that surround the best fit calculated seismic event location may deviate significantly from an elliptical shape. This can be handled using a gridded residuals approach to calculating uncertainties (Willcock and Toomey, 1991). Basically, the approach involves generating a regularly spaced grid of points surrounding the best-fit location found with the least-squares inversion technique and, at each of these points, using a 1D minimization algorithm to find the origin time which yields the smallest sum squared weighted residual between observed and predicted seismic parameters,  $\chi^2$ , at that location.  $\chi^2_{\min}$  is known to us from the least squares algorithm so we can compute  $\Delta\chi^2 = \chi^2 - \chi^2_{\min}$ . Contours of constant  $\Delta\chi^2$  correspond to confidence intervals so from the gridded residuals, we can find the non-linear 95% confidence interval and compare it to the elliptically shaped, linear 95% confidence bounds deduced with the least squares algorithm.

Note that this technique only removes the assumption that the Earth model is linear. The assumption that the data errors are normally distributed remains. To remove this assumption as well will require a full-blown grid search algorithm such as the one developed by Rodi and Toksoz (2001). The advantage of the technique described here is that it does not require computationally expensive Monte Carlo procedures to generate the uncertainty information. While the full grid-search algorithm may take many hours to complete, the grids shown in this paper require at most a couple of minutes to compute. Furthermore, for problems characterized by a single, well defined minimum, the least squares algorithm will find the same  $\chi^2_{\min}$  value, at the same location in space, as the minimum  $\chi^2$  on the grid. This means that we don't have to use the grid to find the best-fit event location, we can leave that to the very efficient least squares algorithm. The grid is used only to characterize the spatial distribution of  $\Delta\chi^2$  surrounding the best fit location. Furthermore, it is not necessary to compute residuals on a full 3D grid in order to illuminate the geometry of the 3D uncertainty distribution. It is frequently sufficient to generate the residuals on 3 mutually orthogonal planes, thereby reducing the computational burden from  $O(n^3)$  to  $O(n^2)$ .

Figure 3 illustrates the gridded residual uncertainty boundaries surrounding the October 25, 2002 Sea of Japan event that was described in an earlier section of this paper. The three plots illustrate the gridded residuals on 2 vertical and 1 horizontal plane, all of which have their origins at the epicenter of the event. In the figure in the upper left, note the substantial difference between the linear (white) and non-linear (black) 95% confidence limits around the best fit event location. In particular notice that while the linear uncertainty ellipsoid does not intersect the Earth's surface,

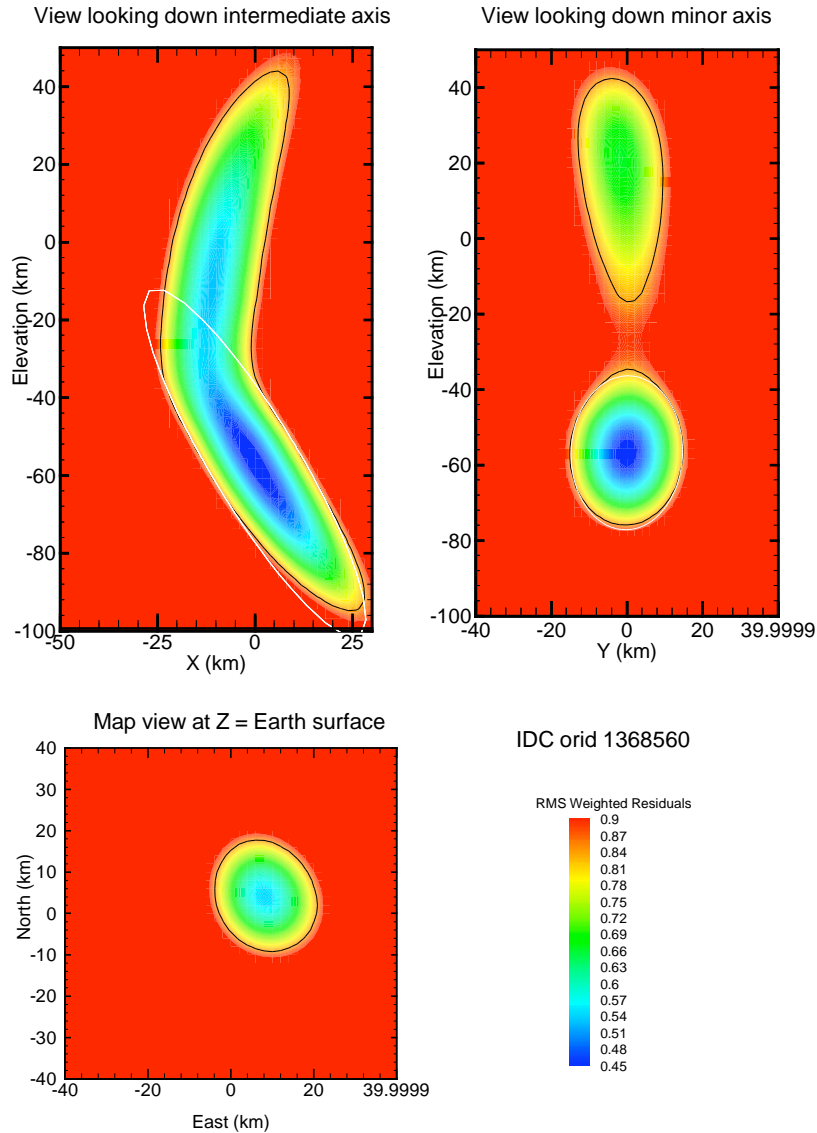


**Figure 3. Gridded residual uncertainties surrounding the October 25, 2002 Sea of Japan event. Colors represent the root mean squared weighted residuals at each point in the figure. The black curve illustrates the non-linear 95% confidence limits surrounding the best fit location, deduced from the gridded residuals. The white curve represents the intersection of the plane of the figure with the linear 3D uncertainty ellipsoid illustrated in Figure 1. The origin of the plots coincides with the epicenter of the event.**

the non-linear uncertainty boundary most decidedly does. In a nuclear monitoring situation, failure to observe the non-linear uncertainty limits would lead investigators to an incorrect conclusion as to whether or not this event could have occurred at the surface. Once again, the non-linearity is most pronounced at the Moho at a depth of 30 km.

### Local Minima

Another challenge in locating seismic events is dealing with the possibility that several local minima may exist in the sum squared weighted residuals. The iterative least squares algorithm can be misled in its quest for the global minimum if the initial guessed starting location for the algorithm lies upgradient from a local rather than the global minimum. While grid search algorithms have a higher probability of finding the global minimum than a simple least

squares algorithm, no algorithm can guarantee with 100% confidence that it will locate the global minimum in a finite number of computations.

LocOO can optionally implement a hybrid least squares – grid search algorithm to improve the probability of finding the global minimum rather than a local minimum. The approach is to specify a number of depths at which the location should be started. The locator performs a fixed depth location at each of the specified depths and then seeks a free depth solution starting at the fixed depth location that provided the lowest sum squared weighted residuals. Then starting from the free depth solution, the locator steps out horizontally a user-specified distance in a number of equally spaced azimuthal directions and repeats the free depth solution. The location found in this manner that has the lowest sum squared weighted residual is accepted as the final best fit location.

By way of an example, the Sea of Japan event that has already been used as an example several times in this paper exhibits a local minimum at a depth of 14 km. For some initial starting locations, this local minimum location is found instead of the presumed global minimum location at 57 km depth. The hybrid least squares – grid search algorithm described above dramatically improves the probability of finding the 57 km depth solution.

### **Fixed Depth Solutions**

The 2D linear uncertainty ellipses that surround fixed depth seismic event locations bear some reconsideration. When designing a solution to a seismic event location problem (or any problem for that matter) it is crucial to first very clearly state the problem that the solution is designed to address. The question that fixed depth solutions address is “if the seismic event occurred at the a particular depth  $Z$ , where in 2D location space did it occur, and what is the uncertainty associated with that location?”

At first this may appear to be a two-dimensional question since only the 2 horizontal components of the event location are explicitly sought. More careful reading of the question reveals, however, that there is at least a suggestion of a third dimension to the question. The first phrase, “If the event occurred at depth  $Z$ , ...”, acknowledges that the event may not have occurred at depth  $Z$ . We are not asserting, with infinite confidence that the event actually occurred at depth  $Z$ . In addition, when we ask “... and what is the uncertainty associated with that location?”, we do not necessarily intend to limit the uncertainty to just the 2 horizontal dimensions. The question would be clearer if it were stated as “If the event occurred at depth  $Z$ , where in 2D horizontal space did it occur and with what probability did it occur there, as opposed to some other position in 3D space?” Current practice answers the question “Given that the event is known with zero uncertainty to have occurred at depth  $Z$ , where in 2D horizontal space did it occur and with what probability did it occur there, as opposed to some other position in 2D horizontal space?”

What is actually desired is a 2 dimensional location at the specified depth, but with uncertainty that considers the vertical dimension as well. This can be accomplished by calculating  $\sigma^2$  using the F-statistic with three free parameters instead of two and by scaling the dimensions of the uncertainty ellipse to reference the global minimum sum squared weighted residuals,  $\sigma^2_{3D,min}$  instead of  $\sigma^2_{2D,min}$ .

When a fixed-depth solution is requested, the least-squares algorithm returns an uncertainty ellipse with the equation

$$c_0x^2 + c_1xy + c_2y^2 = 1 \tag{1}$$

where  $x$  is north in km,  $y$  is east in km, and the coefficients  $c_i$  define the shape of the ellipse. Equation 1 defines the distance from the point in parameter space where  $\sigma^2 = \sigma^2_{2D,min}$  to the elliptical contour in parameter space where  $\sigma^2 = \sigma^2_{2D,min} + 1$ , or,  $\sigma^2 = 1$ . This ellipse is then scaled with two parameters. The first is  $s_D^2$ , the data variance scale factor, which is a constant described by Jordan and Sverdrup (1981) and Bratt and Bache (1988). The second is the F-statistic,  $M' F[M', N, p]$ , where  $M'$  is the number of free parameters in the uncertainty analysis,  $N$  is the number of degrees of freedom (number of observations minus number of free parameters in the location calculation) and  $p$  is the desired confidence level. Note that the number of free parameters in a fixed-depth location calculation is 3, one for each horizontal component of the location and one for the origin time.  $M'$  is the number of free parameters in the uncertainty calculation. In current practice, when calculating the 2D spatial uncertainty ellipses,  $M'$  is set to 2,

one for each of the horizontal coordinates of the location. This implies perfect confidence in the depth of the solution. In current practice, the uncertainty ellipse is given by

$$c_0x^2 + c_1xy + c_2y^2 = s_D^2 2F[2, N, p] \quad (2)$$

which yields an elliptical contour in  $x, y$  space where

$$\sigma^2 = s_D^2 2F[2, N, p] + \sigma_{2D,\min}^2 \quad (3)$$

To obtain an ellipse scaled to include 3D uncertainty information, we wish find the contour where

$$\sigma^2 = s_D^2 3F[3, N, p] + \sigma_{3D,\min}^2 \quad (4)$$

To find this contour centered on  $\sigma_{2D,\min}^2$  we subtract  $\sigma_{2D,\min}^2$  from both sides to obtain

$$\sigma\sigma^2 = \sigma^2 - \sigma_{2D,\min}^2 = s_D^2 3F[3, N, p] + \sigma_{3D,\min}^2 - \sigma_{2D,\min}^2 \quad (5)$$

So, to rescale the uncertainty ellipse to three free parameters centered on  $\sigma_{2D,\min}^2$ , the ellipse should be

$$c_0x^2 + c_1xy + c_2y^2 = s_D^2 3F[3, N, p] + \sigma_{3D,\min}^2 - \sigma_{2D,\min}^2 \quad (6)$$

### Example

Let us compare these approaches by applying them to a sample problem. The location problem that we will address is the India nuclear test of May 11, 1998. Of the 60 travel time observations available for the event, only the 27 observations from stations located in an azimuthal window  $45^\circ$  wide, located to the north of the event have been used. Figure 4a is a vertical cross section through the hypocenter of the event, oriented perpendicular to the trend of the intermediate axis of the 3D hypocentral uncertainty ellipsoid. Figure 4b is a horizontal slice through the epicenter of the event, which is located 40 km above the hypocenter. The colors represent contours of  $\sigma\sigma^2$  measured relative to  $\sigma_{3D,\min}^2$ . The black contour lines represent the 3D, non-linear 95% confidence intervals calculated directly from the gridded residuals. The white ellipses represent the intersections of the 3D, linear 95% hypocentral uncertainty ellipsoid with the plane of the figure. In Figure 4b, the unmodified (Equation 2) and modified (Equation 6) fixed-depth uncertainty ellipses are also illustrated.

Of all the confidence intervals plotted in Figure 4b, the gridded-residuals confidence intervals is the one that best captures the real 3D uncertainty in the event location (assuming that it occurred at the surface). This is because it does not assume that the Earth model used to locate the event is linear. This confidence interval is the only one that is not an ellipse. While it is the best, it is also the most expensive to compute (~ 3 minutes) and the most difficult to process. It is difficult to process because it is not an ellipse and therefore cannot be expressed conveniently in text format but rather must be viewed graphically.

The modified fixed-depth confidence ellipse coincides almost perfectly with the gridded-residuals confidence interval but does not suffer from the disadvantages of the latter. It is quick to compute (~ 1 second) and convenient to process. It is more accurate than the 3D hypocentral ellipsoid intersection because the latter fails to account for non-linearity in the Earth model. The hypocenter of this event was calculated to be at a depth of 40 km, which is below the base of the crust in the IASP91 Earth model. Figure 4a illustrates quite clearly that, while the ellipsoid captures the uncertainty in the mantle with reasonable accuracy, it deviates significantly from the gridded-residuals confidence interval above the crust-mantle boundary where the seismic velocities differ substantially from the velocities in the vicinity of the hypocenter. The modified fixed-depth confidence ellipse reflects conditions at the Earth's surface and hence is not as susceptible to disruption from non-linear effects as is the ellipsoid intersection. If the Earth model were perfectly linear, the ellipsoid intersection ellipse and the modified fixed-depth confidence ellipse would coincide exactly.

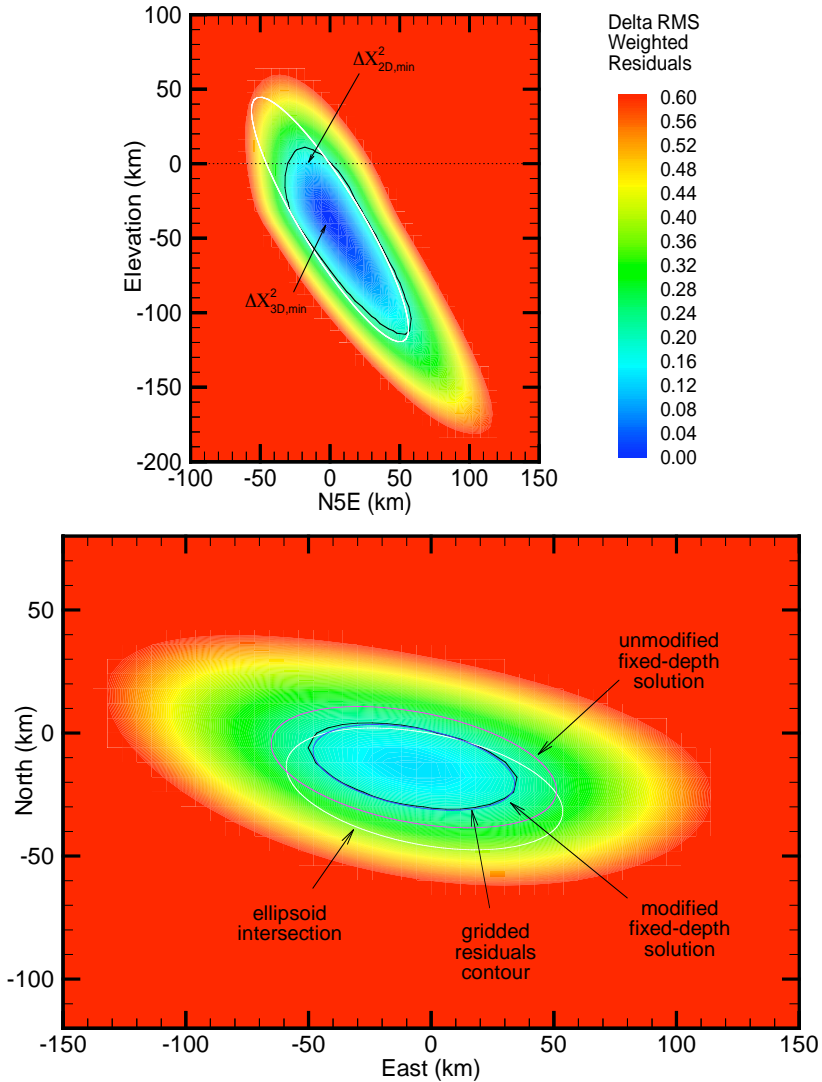


**Figure 4. Uncertainty of fixed depth solutions.**

The unmodified fixed-depth ellipse, like the modified fixed-depth ellipse and the gridded-residuals contour, is centered on  $\chi^2_{2D,min}$ . Its confidence ellipse is substantially larger than the modified fixed-depth ellipse since the unmodified fixed-depth solution is attempting to provide an answer to a different question than is the modified fixed-depth solution. The unmodified fixed-depth ellipse will not always be larger than the modified fixed-depth ellipse. Figure 5 compares the areas of the 3 elliptical confidence intervals as a function of the depth at which the depth is fixed. At depths near the hypocenter, the unmodified fixed-depth ellipse has linear dimensions that are approximately 12% smaller than the modified fixed-depth ellipse reflecting the fact that the F-statistic with 2 free parameters is substantially smaller than the F-statistic with 3 free parameters. While the size of the modified fixed-depth ellipse decreases rapidly with distance from the depth of the hypocenter, the size of the unmodified fixed-depth ellipse remains relatively unchanged, reflecting the fact that the former is centered on  $\chi^2_{3D,min}$  while the latter is centered on  $\chi^2_{2D,min}$ .

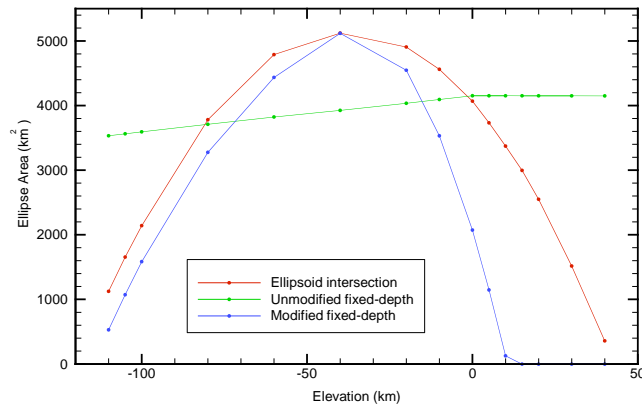


**Figure 5. Comparison of the areas of the 3 elliptical confidence intervals as a function of the depth at which the depth is fixed.**

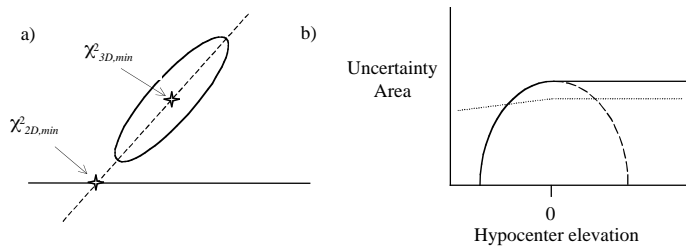


**Figure 6. Sketch illustrating airquake scenarios. In b, the solid curve represents the modified fixed-depth uncertainty ellipse altered to impose the constraint that the event must have occurred below the Earth's surface. The dashed curve represents the modified fixed-depth ellipse not altered to deal with airquakes, and the dotted curve represents the unmodified fixed-depth ellipse.**

### Airquakes

What happens when the hypocenter of the free-depth solution has a negative depth, implying that the event occurred above the surface of the Earth? For the free-depth solution, the unrealistic location and associated uncertainty should be reported as is so that the analyst can gain whatever insight into the problem that they may be able to glean. If the 3D uncertainty limits intersect the surface of the Earth, the results are still useful.

For a fixed-depth solution however,  $\sigma_{3D,min}^2$  now occurs at a location in space that is not possible and it is desirable to mitigate its impact. Figure 6a illustrates an extreme example where even the 3D uncertainty limits of the hypocenter do not intersect the surface. Without further modification, the area of the modified fixed-depth uncertainty ellipse would be zero in this case. This seems unreasonable, because we know that airquakes cannot happen. The event must have occurred somewhere at or below the surface of the Earth, with the most likely location being close to the Earth's surface since this would require the smallest deviation from the best-fit 3D calculated location.

The proposed remedy is based on the premise that the calculated value of  $\sigma_{3D,min}^2$  could not be achieved in reality and hence should not be used to rescale the fixed-depth uncertainty ellipse. Instead,  $\sigma_{3D,min}^2$  should be replaced in Equation 6 with the closest reasonable alternative, which would be  $\sigma_{2D,min,0}^2$ , the minimum value of  $\sigma^2$  found at the Earth's surface. In Figure 6a, this is tantamount to shifting the uncertainty ellipsoid along its major axis until the hypocenter coincides with the Earth's surface. If depth in the fixed-depth solution was fixed at the Earth's surface, this yields an ellipse scale factor of  $s_{\sigma} 3F[3, N, p]$  rather than  $s_{\sigma} 3F[3, N, p] + \sigma_{3D,min}^2 - \sigma_{2D,min}^2$ , regardless of the elevation of the hypocenter above the Earth's surface. Figure 6b illustrates how the ellipse area of a fixed-depth

solution with depth fixed at the surface would change as a function of hypocentral elevation. For airquakes, the modified fixed-depth solution maintains a constant uncertainty ellipse area regardless of the elevation of the hypocenter above the Earth's surface.

To summarize, the modified fixed-depth uncertainty ellipse equation is

$$\begin{aligned} c_0x^2 + c_1xy + c_2y^2 &= s_D^2 3F[3, N, p] + \sigma_{3D, \min}^2 \square \sigma_{2D, \min}^2 & Z_{\text{hypo}} \leq 0 \\ c_0x^2 + c_1xy + c_2y^2 &= s_D^2 3F[3, N, p] + \sigma_{2D, \min, 0}^2 \square \sigma_{2D, \min}^2 & Z_{\text{hypo}} > 0 \end{aligned} \quad (7)$$

where  $Z_{\text{hypo}}$  is the elevation of the event hypocenter above the Earth's surface.

## **CONCLUSIONS AND RECOMMENDATIONS**

A number of improvements to current seismic event location capabilities have been described. These include: a) the addition of the ability to compute multidimensional uncertainty boundaries, b) alternative methods of dealing with non-linear Earth models, which improve the convergence behavior of the least squares algorithm and which give greater insight into the non-linear uncertainty in the computed location, c) addition of optional algorithms for improving the probability that the global, rather than local minima are found, and d) an alternative method for scaling the dimensions of 2D fixed-depth uncertainty intervals such that they reflect uncertainty in depth as well as horizontal components. All of these capabilities are available in a new location code called LocOO.

## **REFERENCES**

- Ballard, S., 2002, Seismic Event Location Using Levenberg-Marquardt Least Squares Inversion, Sandia National Laboratories Report, SAND2002-3083.
- Bratt, S. R. and T. C. Bache (1988), Locating Events with a Sparse Network of Regional Arrays, Bull. Seis. Soc. Am., v. 78, pp. 780-798.
- Geiger, L. (1910), Herdbestimmung bei erdbeben ans den ankunftszeiten, K. Gessel. Wiss. Goett. v. 4, pp. 331-349.
- Jordan, T. H. and K. A. Sverdrup, 1981, Teleseismic Location Techniques and their Application to Earthquake Clusters in the South-Central Pacific, Bull. Seis. Soc. Am., v. 71, pp. 1105-1130.
- Levenberg, K., 1944, A method for the solution of certain non-linear problems in least squares, Quart. Appl. Math., v. 2, pp. 164-168.
- Marquardt, D. W., 1963, Journal of the Society for Industrial and Applied Mathematics, v. 11, pp. 431-441.
- Press, W. H., S. A. Teukolsky, W. T. Vetterling and B. P. Flannery, 2002, *Numerical Recipes in C++*, *The Art of Scientific Computing*, 2<sup>nd</sup> Edition, Cambridge University Press.
- Rodi, W. and M. Toksoz, 2001, Uncertainty Analysis in Seismic Event Location, Proceedings of the 23<sup>rd</sup> Seismic Research Review, pp. 324-332.
- Wilcock, W. S. D. and D. R. Toomey, 1971, Estimating Hypocentral Uncertainties for Marine Microearthquake Surveys: A Comparison of generalized inverse and grid search methods, Marine Geophysical Researches, v. 13, 161-171.